RESEARCH PAPER

A Study of the Influence of Percentage of Copper on the Structural and Optical Properties of Au-Cu Nanoparticle

Parivash Mashayekhi Shams [1 *], Mirabdollah Seyed Sadjadi [1] and Alireza Banaei [2]

[1] Department of Chemistry, Science and Research Branch, Islamic Azad University, Tehran, Iran

[2] Department of Chemistry, Payame Noor University, Tehran, Iran

ARTICLE INFO

Article History:
Received 21 February 2016
Accepted 14 April 2016
Published 1 July 2016

Keywords:
Au-Cu nanoparticle
Optical properties
Percentage of copper
Structural

ABSTRACT

Here we present our experimental results in synthesizing Au-Cu nano-particles with tunable localized surface plasmon resonance frequency through wet-chemical at temperature room. The reaction is performed in the presence of ascorbic acid as a reducing agent and polyvinyl pyrrolidone as capping agent via four different procedures: (1) mixture of 90% $HAuCl_4$ and 10% $CuSO_4.5H_2O$ precursors, (2) mixture of 75% $HAuCl_4$ and 25% $CuSO_4.5H_2O$ precursors, (3) mixture of 50% $HAuCl_4$ and 50% $CuSO_4.5H_2O$ precursors (4) mixture of 25% $HAuCl_4$ and 75% $CuSO_4.5H_2O$ precursors. Effect of different percentages of Cu on Au nanoparticles has been analyzed using X-ray diffraction (XRD), scanning electron microscopy (SEM with EDAX analysis), DRS UV-Vis, and Fourier transform IR spectra (FTIR) analysis. X-ray diffraction (XRD) analysis revealed that the nanoparticles are of cubic structure without an impure phase. The successful doping of the Cu into the Au host was evident by XRD line shiftings. The increasing percentage of copper leads to the decreasing grain size. With the increase of Cu^{2+} to Au^{3+} ratio in the Cu^{2+}/Au^{3+} mixed solution (> 50% Cu), XRD lines show no shifting. The average crystal sizes of the particles at room temperature were less than 9.9 nm. The surface plasmon resonance peak shifts from 380 to 340 nm, party due to the change in particle size. SEM images show a spherical shape and the size of nanoparticles becomes smaller with increasing the percentage of copper. Moreover, in the molar ratio of Cu^{2+}/Au^{3+} = 75/25 (>50% Cu), mixture of spherical and trigonal nanoparticles were prepared. Fourier transform infrared spectroscopy (FT-IR) showed the coordination and conjugation nanoparticles with N and O atoms of C-N and C=O bonds.

How to cite this article
Mashayekhishams P, Seyed Sadjadi M, Banaei A. A Study of the Influence of Percentage of Copper on the Structural and Optical Properties of Au-Cu Nanoparticle. Nanochem Res, 2016. 1(2): 143-149. DOI: 10.7508/ncr.2016.02.001

INTRODUCTION

Over the last years, nanomaterials have become significant scientific fields. The significance of these research fields relies upon the new properties of materials provided by structures of size in the nanometric scale. Materials of this kind can be effective in many applications, such as optical sensors, biomedical sensors, chemical catalysis and optoelectronic devices, among others [1-5]. Since the optical properties are dependent on the frequency at which the surface plasmon resonance (SPR) arises [6], the capability to change the SPR frequency is of major importance. As, plasmon resonances in the metal nanoparticles forcefully depend on the particle size and morphology of the nanoparticles [7-8]. Control above these parameters should let tuning the LSPR energy with respect to the start of inter band transitions. Size-controlled synthesis of nanoparticles is a main step in the expansion of new nanotechnology applications because the potential applications and their yield strongly depend on the following parameters: i) excellent size control, ii) Combinational control [9-12]. As well as the SPR frequency of metal

* Corresponding Author Email: *prmashayekhi@gmail.com*

nanoparticles can be varied by the linkage another metal element in it [6]. Gold nanoparticles have possessed considerable attention owing to their unique electronic and optical properties, as well as their major potential for medical applications [13-15]. Nowadays, gold nanostructures have been also engaged, for their feasible applications, in photothermal therapy, radiotherapy and cancer cell imaging because of their good biocompatibility [16-18]. Doping Au by other metals provides an available route to modulate electronic and optical properties [19]. Here, we synthesized Au-Cu nanoparticles (10%, 25%, 50%, 75% Cu), then studied structural and optical properties of them. In this new nanoparticles, the SPR frequency can be regulated in the range from SPR frequency can be modulated in the range from SPR frequency of Au and Cu nanoparticles by varying the concentration of Au/Cu molar ratio.

EXPERIMENTAL

Material

All of the chemicals were analytical grade and were used as purchased without further purification. Copper(II) sulfate pentahydrate salt ($CuSO_4.5H_2O$) was 98% pure (Merck), Gold(III) chloride trihydrate ($HAucl_4.3H_2O$) was purchased from sigma Aldrich. Polyvinlpyrrolidone (PVP, average molecular weight of 30000) from TCI America was used as the capping agent. Ascorbic acid (99.7%, Merck), and sodium hydroxide NaOH (> 98%, Merck) were also used to adjust the pH. Aqueous solutions were made in deionized water.

Method

All glassworks were cleaned with an aqua regia solution (3:1, HCl:HNO_3), and then washed. In this work, at the first time, we prepared four solutions namely 0.05 M $HAuCl_4.3H_2O$ (Solution A), 0.0087 M $CuSO_4.5H_2O$ (Solution B), 0.026 M $CuSO_4.5H_2O$ (Solution C), 0.078 M $CuSO_4.5H_2O$ (Solution D), 0.23 M $CuSO_4.5H_2O$ (Solution E). These were used in preparing Au-Cu precursor solutions with different ratios as shown in Table 1. Composition of solutions A and B is labeled as concentration1, solutions A and C is labeled as concentration 2, solutions A and D is labeled as concentration 3, solutions A and E is labeled as concentration 4. 0.001 M PVP polymer solution was used the synthesis. Then, with constant stirring and under N_2 atmosphere mixture of ascorbic acid (0.2 M) and sodium hydroxide (0.2 M) was added to the synthesis solution. Color change occurred in the aqueous phase to black. When color of the solution did not change, the reaction was ceased. After separation from the mixed solution, the precipitation washed 3-4 times by de-ion water and the 2-3 times by ethanol. The powder of Au-Cu nanoparticles was characterized by scanning electron microscopy (SEM with EDAX), X-ray diffraction (XRD), Fourier transform IR spectra (FTIR) and DRS UV-Vis spectroscopy. X-ray powder diffraction (XRD) analysis was performed on a D5000-siemens with Cu Kα radiation (λ = 1.541 A˚) using a 30 kV operation voltage and 40 mA current. Scanning electron microscopy (SEM) images were obtained using a LEO 1430 VP microscopy. DRs UV-Vis spectra of the synthesized materials were recorded in the scan range 200-1000 nm, using a UV-Vis spectrophotometer (S-4100, scinc Korea). Infrared (IR) spectrum was measured on a Perkin Elmer RXI fourier transform infrared (FTIR) spectrometer.

RESULTS AND DISCUSSION

SEM Characterization

The nanostructures of the samples are certified by using SEM micrographs as shown in Fig. 1. (SEM with EDAX analysis). Figs. (1a, c, e) displayed spherical morphology with different particles sizes. It can be seen from these pictures that the particle size decreased with the increase of copper percentage. When molar ratio of Cu^{2+}/Au^{3+} = 75/25 (>50%), mixture of spherical and trigonal nanoparticles was prepared (Fig. 1g). Figs. (1b, d, f, h) show the EDAX spectrum of Au-Cu nanoparticles with 1.64% copper and 91.54% gold (for 10% Cu), 2.05% copper and 92.85% gold

Table 1. Au-Cu Precursor Solutions with Different Ratios

Au-Cu	$HAuCl_4$ solution	$CuSO_4.5H_2O$ solution	PVP solution	Ascorbic acid solution	Sediment color
90:10	0.05	0.0087	0.001	0.2	Black
75:25	0.05	0.026	0.001	0.2	Black
50:50	0.05	0.078	0.001	0.2	Black
25:75	0.05	0.230	0.001	0.2	Black

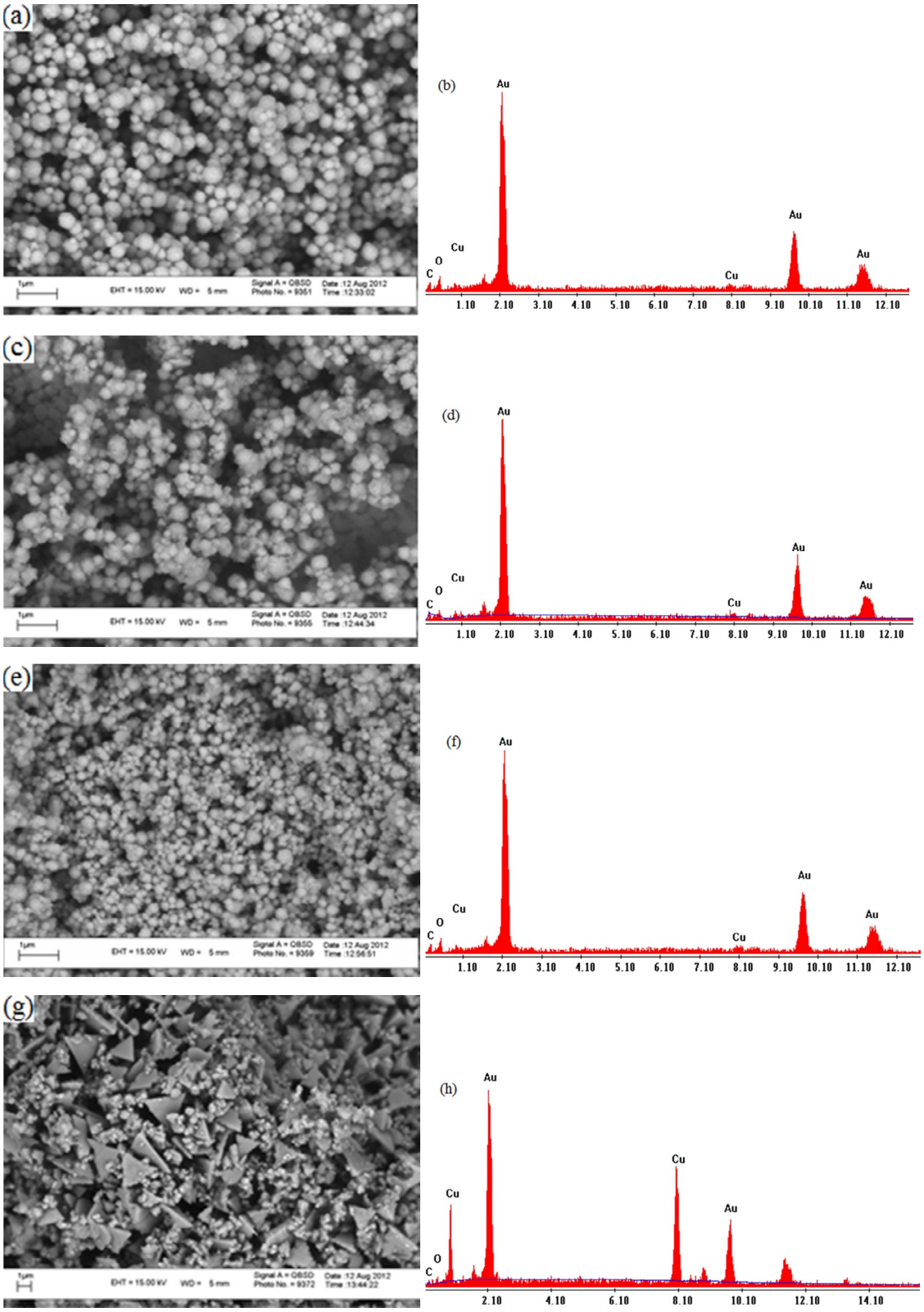

Fig. 1. (a, c, e, g) SEM images of Au-Cu nanoparticles: (a) 10 at%, (c) 25 at%, (e) 50 at% (g) 75 at%. (b, d, f, h) EDAX Spectrum of Au-Cu nanoparticles: (a) 10 at%, (c) 25 at%, (e) 50 at% (g) 75 at%.

Table 2. Particle Size Variation with Different Percentages of Copper from XRD Analysis

	Cu (10%)	Cu (25%)	Cu (50%)
Particles size (nm)	9.9	4.7	4.5

(for 25% Cu), 1.02% copper and 92.16% gold (for 50% Cu), 29% copper and 67% gold (for 75% Cu) were estimated from EDAX analysis. The EDAX spectrum of Au-Cu nanoparticles illustrate that Au is a major element. Further confirmed the successful doping of Cu in the Au host structure.

XRD Diffraction Analysis

The structures of the Au-Cu nanoparticles with different percentages of Cu have been studied at room temperature using X-ray diffractometer. The XRD patterns of pure Au, Au-Cu nanoparticles is shown in Fig. 2. As no extra peak was observed in the XRD pattern, clearly this indicated the phase purity and absence of impurity phases. All the diffraction peaks can be well indexed to face-centered cubic (FCC) Au according to the JCPDS card (NO.1-1172). Four pronounced Au diffraction peaks (111), (200), (220) and (311) appear at 2θ = 38.39˚, 44.9˚, 64.9˚ and 78˚, respectively. The four most intense peaks of the XRD pattern of sample show a slight shifting of the center of the diffraction peaks toward a high angle (Fig. b, c, d). The shifting of the XRD lines suggests that Cu has been successfully substituted in to Au host structure at the Au site. The average crystallite size can be calculated from the full width at half maximum (FWHM) of the diffraction peaks using the debye-scherer formula:

$$D = 0.9\lambda/\beta\cos\theta \quad (1)$$

Here, D is the mean grain size, λ is the X-ray wavelength, β is the full width of half maximum intensity of diffraction line and θ is the diffraction angle. The grain size of the samples was calculated from Eq. (1) using (111) reflection in XRD pattern. The values of particle size for different percentages of copper are listed in Table 2, from which it is clear that the particle size decreases with increasing percentage of copper.

With the increase of Cu^{2+} to Au^{3+} ratio in the $Cu^{2/+}Au^{3+}$ mixed solution (>50% Cu), XRD lines show no shifting. No shifting of the XRD lines suggests that Cu has not been doped in Au (Fig. 2e).

DRS UV-Vis Spectra

The DRS UV-Vis spectra of Au-Cu nanoparticles were recorded for all the samples having different percentages of Cu impurity from 10% to 50%. Fig. 3 shows the UV-Vis absorption spectrum of as-prepared pure Au, pure Cu, 10% Cu, 25% Cu, 50% Cu. It exhibits an intense peak centered at 380 nm and another peak with low intensity at 480 nm as shown in Fig. 3. Strong peak due

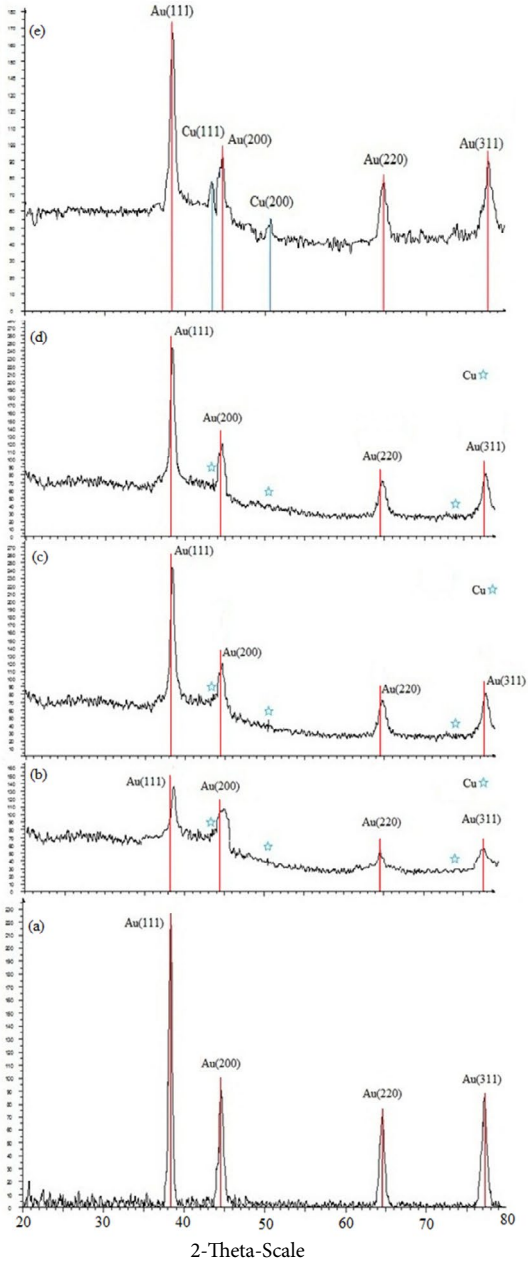

Fig. 2. X-ray diffraction patterns of the (a) pure Au, (b) 90% Au, (c) 75% Au, (d) 50% Au, (e) 25% Au.

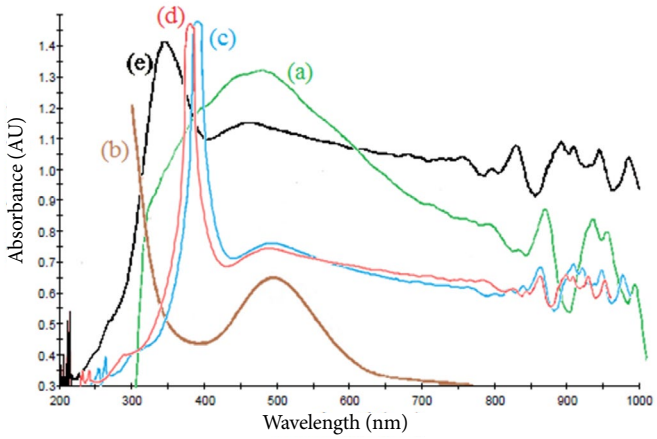

Fig. 3. Optical absorption spectrum of (a) Pure Au, (b) Pure Cu, (c) 10% Cu, (d) 25% Cuand (e) 50% Cu.

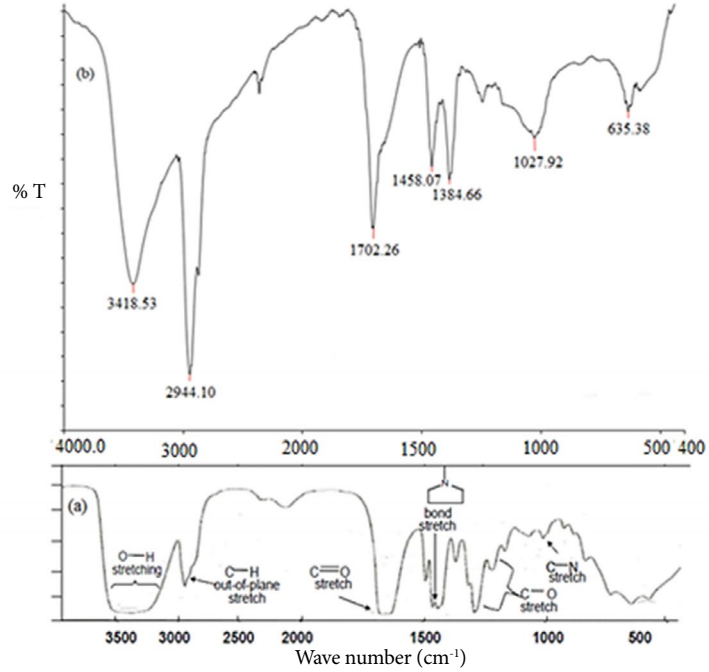

Fig. 4. FTIR spectrum for (a) Pure PVP [20] and (b) PVP-50% Cu.

to Au-Cu nanoparticles that the blue shift in the absorption band edge with increase percentages of copper due to smaller particle sizes in the study. In this nanoparticles, the SPR frequency can be modulated in the range from SPR frequency of Au nanoparticles, by changing the percentages of Cu, and hence, is controlled. As clearly shown in Fig.3 the absorption edges reveal a large shifting (40 nm) with increasing percentage of copper. A weak peak around 500 nm appeared to be due to copper nanoparticles that had been not introduced in the structure of gold nanoparticles.

FTIR Analysis

FTIR spectroscopy was used to analyze the interaction between the metal and PVP. Fig. 4 shows the FTIR spectrum for pure PVP [20] and PVP cladded nanoparticles (for 50% Cu). The FTIR spectrum for pure PVP clearly illustrates that the observed absorption peaks correspond to the characteristic chemical bonds present in PVP. The peak at 1019 cm^{-1} representing the functional unit C-N present in PVP, shifts to 1027.92 cm^{-1} after embedding of nanoparticles. Another peak at 1665 cm^{-1} in pure PVP due to C=O bonds becomes

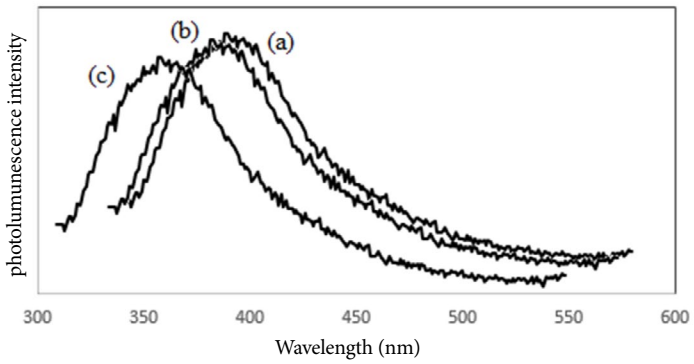

Fig. 5. Photoluminescence spectra for Au-Cu nanoparticles: (a) 10%, (b) 25%, (c) 50%.

narrower and shifts to 1702.26 cm^{-1} after embedding of nanoparticles. This confirms the coordination and conjugation nanoparticles with N and O atoms of C-N and C=O bonds.

Photoluminescence

Photoluminescence study using the 350 nm excitation is reported for the Au-Cu nanoparticles. Typical profiles of the PL spectra are shown in Fig. 5. The results show that the strong emission peaks are observed at 398 nm (50% Cu), 410 nm (25% Cu), 425 nm (10% Cu). It is found that all the PL peaks in Au-Cu nanoparticles have red shifts.

CONCLUSIONS

Au-Cu nanoparticles with various percentages of Cu were successfully synthesized at room temperature by wet-chemical method. The diffraction analysis reveals that Cu doped Au nanoparticles exhibits cubic structure with (111), (200), (220) and (311) planes. XRD and EDAX analyses confirmed that Cu was successfully doped into Au lattice. With the increase of Cu^{2+} to Au^{3+} ratio in the Cu^{2+}/Au^{3+} mixed solution (>50% Cu), XRD lines show no shifting. No shifting of the XRD lines suggests that Cu has not been doped in Au. Absorption edge of Au-Cu nanoparticles showed blue shift due to smaller particle sizes in the study. In these nanoparticles, the SPR frequency can be changed in the range from SPR frequency of Au nanoparticles, by changing the percentages of Cu, and hence, is controlled.

REFERENCES

[1] Puntes VF, Krishnan KM, Alivisatos AP. Colloidal nanocrystal shape and size control: The Case of Cobalt. Science. 2001; 291 (5511): 2115-7.

[2] Somorjai GA, Park JY. Colloid science of metal nanoparticle catalysts in 2D and 3D structures. Challenges of nucleation, growth, composition, particle shape,size control and their influence on activity and selectivity. Top. Catal. 2008; 49 (3): 126-35.

[3] Lara HH, Ixtepan-Turrent L, Garza-Treviño EN, Rodriguez-Padilla C. PVP-coated silver nanoparticles block the transmission of cell-free and cell-associated HIV-1 in human cervical culture. J. Nanobiotechnol. 2010; 8 (1): 1-11.

[4] Rodriguez-Gattorno G, Diaz D, Rendon L, Hernandez-Segura G. Metallic nanoparticles from spontaneous reduction of silver(I) in DMSO. Interaction between nitric oxide and silver nanoparticles. J. Phys. Chem. B. 2002; 106 (10): 2482-7.

[5] Burda C, Chen X, Narayanan R, El-Sayed MA. Chemistry and properties of nanocrystals of different shapes. Chem. rev. 2005; 105 (4): 1025-102.

[6] Magruder RH, Zuhr RA. Formation and optical characterization of nanometer dimension colloids in silica formed by sequentially implanting in and Ag. J. Appl. Phys. 1995; 77 (7): 3546-8.

[7] Kelly KL, Coronado E, Zhao LL, Schatz GC. The optical properties of metal nanoparticles: The influence of size, shape, and dielectric environment. J. Phys. Chem. B. 2003; 107 (3): 668-77.

[8] Jin M, He G, Zhang H, Zeng J, Xie Z, Xia Y. Shape-controlled synthesis of copper nanocrystals in an aqueous solution with glucose as a reducing agent and hexadecylamine as a capping agent. Angew. Chem. Int. Edit. 2011; 50 (45): 10560-4.

[9] Ramos-Delgado NA, Hinojosa-Reyes L, Guzman-Mar IL, Gracia-Pinilla MA, Hernández-Ramírez A. Synthesis by sol-gel of WO_3/TiO_2 for solar photocatalytic degradation of malathion pesticide. Catal. Today. 2013; 209: 35-40.

[10] Medina-Ramírez I, Liu JL, Hernández-Ramírez A, Romo-Bernal C, Pedroza-Herrera G, Jáuregui-Rincón J, et al. Synthesis, characterization, photocatalytic evaluation, and toxicity studies of TiO_2-Fe^{3+} nanocatalyst. J. Mater. Sci. 2014; 49 (15): 5309-23.

[11] Sathishkumar P, Mangalaraja RV, Rozas O, Mansilla HD, Gracia-Pinilla M, Meléndrez MF, et al. Sonophotocatalytic degradation of Acid Blue 113 in the presence of rare earth nanoclusters loaded TiO_2 nanophotocatalysts. Sep. Purif. Technol. 2014; 133: 407-14.

[12] De Toro JA, Andrés JP, González JA, Riveiro JM, Estrader M, López-Ortega A, et al. Role of the oxygen partial pressure in the formation of composite Co-CoO nanoparticles by reactive aggregation. J. Nanopart. Res. 2011; 13 (10): 4583-90.

[13] Huang X, El-Sayed IH, Qian W, El-Sayed MA. Cancer cell imaging and photothermal therapy in the near-infrared region by using gold nanorods. J. Am. Chem. Soc. 2006; 128 (6): 2115-20.

[14] James FH, Daniel NS, Henry MS. The use of gold nanoparticles to enhance radiotherapy in mice. Phys. Med. Biol. 2004; 49 (18): N309.

[15] Wu D, Zhang X-D, Liu P-X, Zhang L-A, Fan F-Y, Guo M-L. Gold nanostructure: Fabrication, surface modification, targeting imaging, and enhanced radiotherapy. Curr. Nanosci. 2011; 7 (1): 110-8.

[16] Murphy CJ, Gole AM, Stone JW, Sisco PN, Alkilany AM, Goldsmith EC, et al. Gold nanoparticles in biology: Beyond toxicity to cellular imaging. Accounts Chem. Res. 2008; 41 (12): 1721-30.

[17] Zhang X-D, Wu H-Y, Wu D, Wang Y-Y, Chang J-H, Zhai Z-B, et al. Toxicologic effects of gold nanoparticles in vivo by different administration routes. Int. J. Nanomed. 2010; 5: 771.

[18] Zhang X-D, Guo M-L, Wu H-Y, Sun Y-M, Ding Y-Q, Feng X, et al. Irradiation stability and cytotoxicity of gold nanoparticles for radiotherapy. Int. J. Nanomed. 2009; 4: 165.

[19] Guo J-J, Yang J-X, Die D. First principle calculation on Au_nAg_2 (n = 1~4) Clusters. Commun. Theor. Phys. 2007; 48 (2): 348.

[20] Khanna PK, Gokhale R, Subbarao VVVS. Poly(vinyl pyrolidone) coated silver nano powder via displacement reaction. J. Mater. Sci. 2004; 39 (11): 3773-6.